

EFSUMB Course Book, 2nd Edition

Editor: Christoph F. Dietrich

Ultrasound of the renal vessels

Boris Brkljačić¹, Colin Deane³, Laurence Needleman, Sergio Castellani⁴, Christoph F. Dietrich⁵

¹Department of Diagnostic and Interventional Radiology, University Hospital "Dubrava", Medical School, University of Zagreb, Zagreb, Croatia

²Vascular Laboratory, Department of Medical Engineering and Physics, King's College, London, UK

³Department of Radiology, Sidney Kimmel Medical College, Thomas Jefferson University, Philadelphia, Pennsylvania, USA

⁴Department of Medical and Surgical Critical Care A.O.-U. Careggi, Associate Professor in Cardiovascular Diseases, Chair of Angiology, University of Florence, Florence, Italy

⁵Department Allgemeine Innere Medizin, Kliniken Beau Site, Salem und Permanence, Hirslanden, Berne, Switzerland

Corresponding author

Acknowledgment: None

Introduction

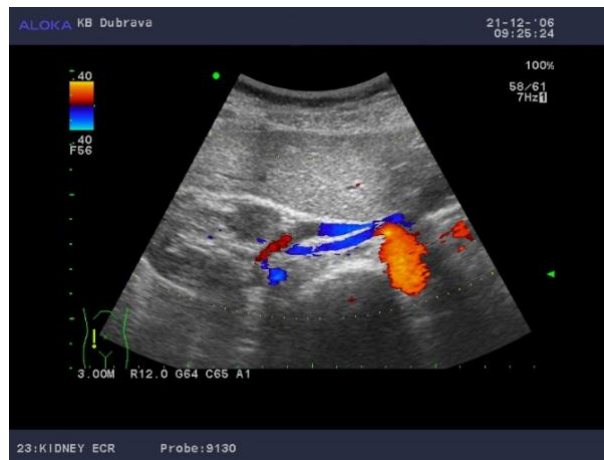
Ultrasound is the most frequently used diagnostic test for the urinary system. B-mode ultrasound allows the evaluation of morphology and kidney anatomy and position, measurement of thickness, assessment of parenchymal echogenicity, and dilatation of the collecting system. Colour duplex Doppler and power Doppler ultrasound of the renal and intrarenal vessels also provide information on renal function, measuring blood flow in renal and intrarenal arteries and veins and permitting evaluation of renal vascular resistance.

Doppler examination technique for renal vessels

Duplex Doppler is used to analyse the flow in the main renal artery and renal vein, as well as intrarenal segmental, interlobar and arcuate arteries and veins. It allows the simultaneous evaluation of kidney morphology and blood flow (color Doppler) with spectral Doppler waveform analysis and quantification [(1, 2)]. Doppler examination of the main renal artery and renal vein is initially performed with the patient supine or side of interest turned up.. In an axial section, the right renal artery origin (from the aorta) is positioned anterolaterally, and the left renal artery origin is positioned posterolaterally [Figure 1]. The lumbar arteries arise posterolaterally. The renal vessels also travel posterolaterally but to the renal hilum.

Figure 1 Transverse scan of the origin of the right renal artery from the aorta, originating anterolaterally. Colour Doppler demonstrates flow away from the transducer, seen in red in the initial, short segment of the artery, courses anteriorly, while

the major part of artery is shown in blue, in which the flow is directed away from the transducer, posterolaterally, towards the right kidney.



The right renal artery is seen behind the inferior vena cava (IVC). The IVC can serve as an acoustic window. With the patient scanned in longitudinal orientation, the retrocaval right renal artery is perpendicular to the image plane and seen as a round structure. The transducer can be slowly rotated so that the right renal artery can appear in long axis. Multiple renal arteries [Figure 2] and early branching of renal artery [Figure 3] can be detected in this fashion.

Figure 2 Longitudinal scan through the IVC. Two right renal arteries are visible behind IVC, in transverse section. The wider renal artery (RA) is superior to the narrow accessory inferior artery.

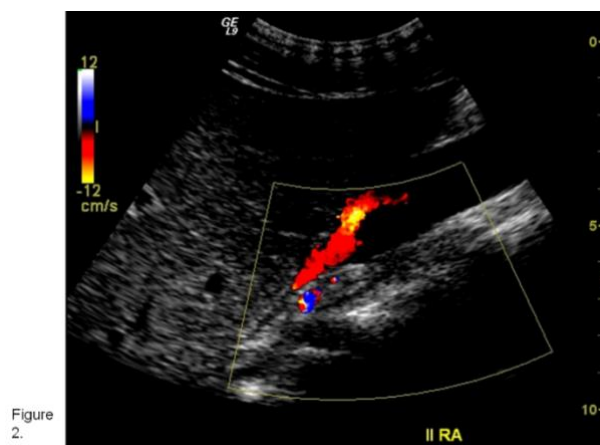


Figure 2.

Figure 3 Early branching of the right renal artery on segmental branches. The artery is easily seen behind the inferior vena cava.

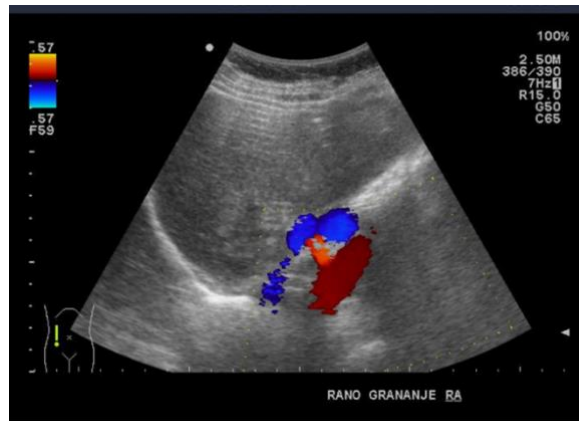


Figure 3

The left renal artery is demonstrated behind the left renal vein. Veins are normally positioned anterior to arteries. Scanning posteriorly or posterolaterally creates the smallest possible insonation angle for renal artery interrogation. In 3–4% of people the right renal artery is preaortic. It is also common to observe a retroaortic or circumaortic left renal vein (Figure 5).

Figure 4 Longitudinal scan through the inferior vena cava (flow seen in blue). Right renal artery (transverse section, flow seen in red) is positioned anterior to IVC (a). In the same patient, the longitudinal section through the anterocavally positioned right renal artery. Spectral waveform confirms arterial flow (b).

a

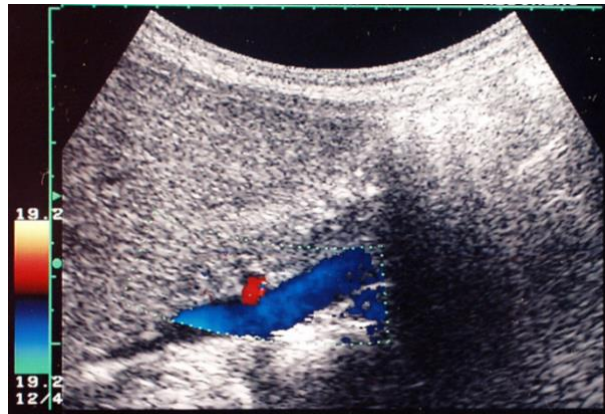


Figure 4a

b

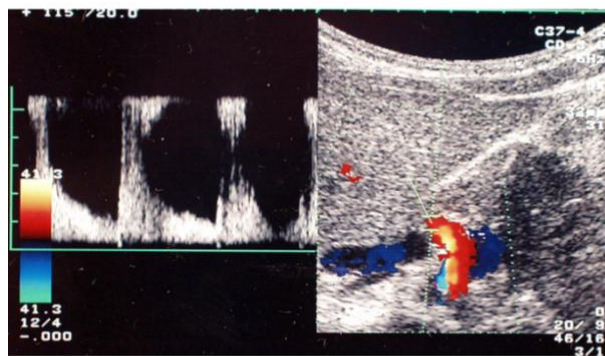


Figure 4b.

Figure 5 Retroaortic position of the left renal vein.

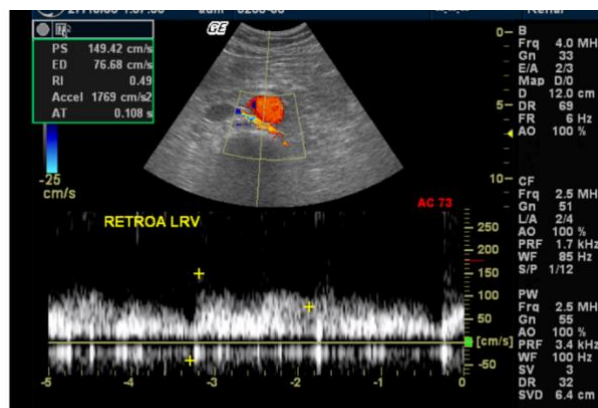


Figure 5.

The left renal vein normally passes between the aorta and superior mesenteric artery. If the angle between these two arteries is small, the left renal vein may be compressed between them. This may cause obstruction, the distal part of left renal vein is dilated. This “nutcracker syndrome” typically causes loin pain and haematuria (also known as, loin pain haematuria syndrome) [(3, 4)]. Doppler spectra in renal and intrarenal arteries have high, continuous, antegrade diastolic flow and short acceleration time. A filled systolic window (spectral broadening) depends on the size of the artery, the curvature of the vessel and the size of the sample volume [Figure 6].

Figure 6 Normal spectral display of flow in the right renal artery. Low-resistance type spectrum is above the baseline, with PSV of 80 cm/s. Angle correction is performed.

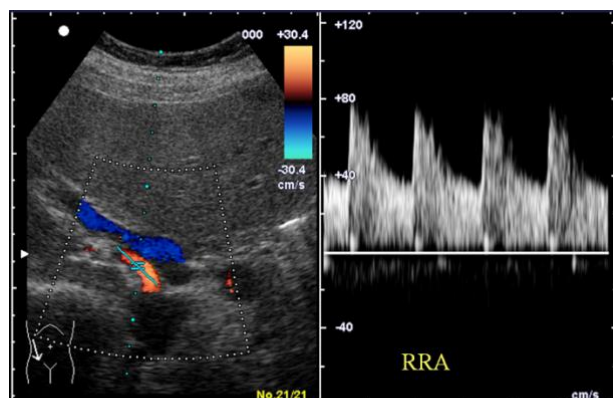


Figure 6.

The renal vein flows in an opposite direction to the renal artery, which is easily visible with colour duplex Doppler. Venous spectra are continuous or with slight respiratory variations [(1, 2)]. Doppler examination of intrarenal vessels should be performed in the lateral decubitus position with a posterior approach, typically with angles less than 30 degrees. Segmental, interlobar and arcuate arteries and veins can be evaluated [Figure 7 and Figure 8] [(1, 2)]. Power-Doppler is sensitive for visualising slow flow in small vessels, and allows the visualisation of flow as far as the renal capsule and visualisation of the interlobular arteries.

Figure 7 Normal intrarenal vessels demonstrated with colour Doppler. Arteries are seen in red and veins in blue dependent on the direction of flow and orientation to the beam.



Figure 7

Figure 8 Normal intrarenal flow demonstrated with e-flow.

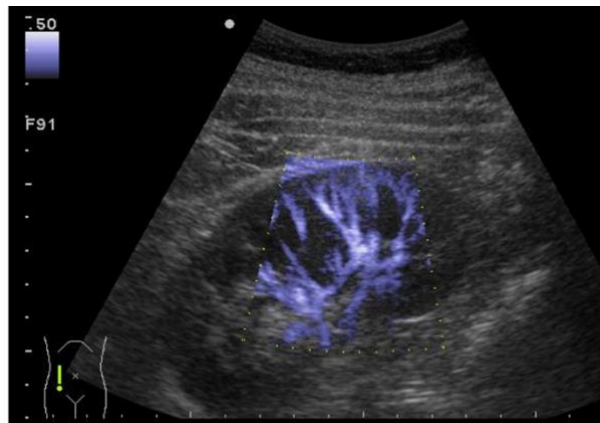


Figure 8

Spectral Doppler of arteries are obtained at typical locations: segmental in the sinus, interlobar on corticocentral junction and corticomedullary borders, and arcuate at the base of the medullary pyramids. Velocities decrease distally. To perform optimal spectral analysis and accurate measurements the wall-filter should be adjusted to the smallest possible values so as not to eliminate low diastolic flow. The lowest pulse repetition frequency should be used

so that aliasing does not occur [(1, 2, 5, 6)]. Doppler spectra can measure resistance index (RI), which reflects renal vascular resistance (RVR). RI is calculated as: $(\text{maximum systolic velocity} - \text{end diastolic velocity}) / \text{maximum systolic velocity}$. Normal values of RI in most studies are in the range of 0.58–0.64 [(5, 7-9)]. We observed normal RI values in adults of 0.60 ± 0.03 [(9)]. Aging renal vasculature is associated with increase in resistance, which is physiological phenomenon and this increase is not accompanied with changes of serum creatinine or creatinine clearance. Therefore older people have 10–15% higher values of RI compared with younger adults. In children values of RI are higher in the first 2 years of life, and between 2 and 6 years of age gradually become similar to adult values [(7, 8)]. For adults, a threshold RI value of 0.70 is an indicator of normal RVR, and all values above 0.70 indicate increased RVR, which is important in evaluation of many pathological conditions, particularly renal parenchymal diseases [(2, 6)]. In children below the age of 6 years threshold values of RI should not be used [Figure 10] [(7)]. Acceleration time (AT), time from the beginning of systole to the systolic peak, can also be measured. RI and AT do not require angle correction. Normal AT is below 0.07 s. Acceleration index (AI) does require angle correction, it is the slope of the early systolic part of the spectrum. The AI is measured at the fastest moving portion of the early waveform before the edge of the waveform bends. The fastest slope generally occurs before peak systole [Figure 9] [(1, 2, 6)]. Normal AI is greater than 3 m/s/s.

Figure 9 Normal Doppler spectrum in interlobar artery with RI=0.56. Below the baseline a continuous spectrum from interlobar vein is visible.

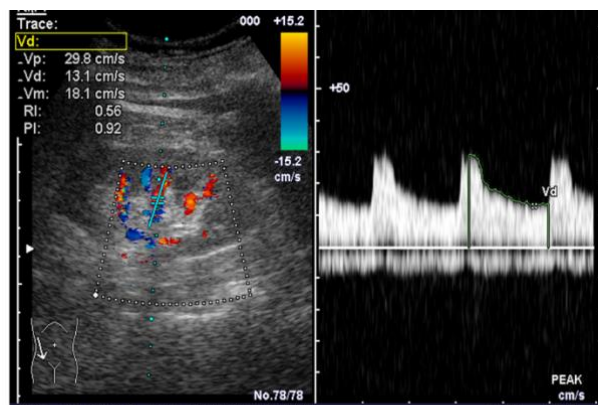


Figure 9.

The diagnosis of renal artery stenosis requires measurement of peak systolic velocity (PSV). PSV in the main renal artery is approximately 1 m/s, and values below 1.5 m/s are still within the normal range.

Figure 10 Normal Doppler spectrum in interlobar artery of a 16-month-old child with RI of 0.74, which is a normal value for this age.

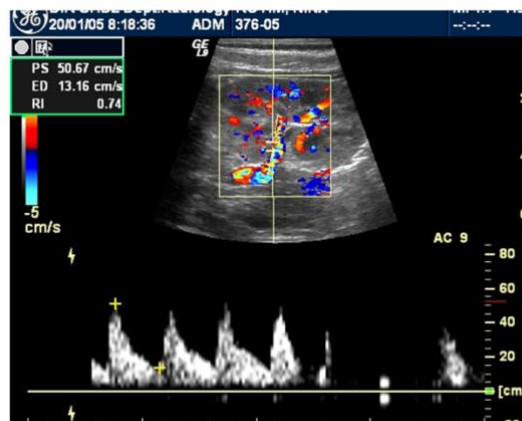


Figure 10.

Renal vascular diseases and renovascular hypertension

Renal vascular diseases include: renovascular hypertension, nephroangiosclerosis, vasculitis (polyarteritis nodosa, granulomatosis with polyangiitis, etc., thrombotic microangiopathies (haemolytic-uraemic syndrome, thrombotic thrombocytopenic purpura), scleroderma, renal infarcts, cortical necrosis, and toxæmia of pregnancy [(10, 11)]. Renovascular hypertension (RVHT) is caused by atherosclerotic stenosis of the renal artery. RAS causes increased production of renin, angiotensin II and aldosterone. It is considered that a more than 60–70% stenosis is needed to produce RVHT. An ischaemic kidney retains sodium and fluid, and longstanding hypertension damages intrarenal vessels. RVHT is clinically significant, but the prevalence of RVHT in the general population of hypertensive patients is very low, only 2–6%. Clinical signs suggesting RVHT include uncontrolled hypertension on multiple medications,

sudden onset of diastolic hypertension, flash pulmonary edema, retinopathy, and hypertension with coronary artery disease [(12-14)]. An important finding is asymmetry of kidney dimensions on ultrasound, CT or MRI [(10, 11)]. Atrophy may predict an inadequate response to revascularization. The presence of RAS does not imply that the patient has RVHT; asymptomatic RAS is common and more than 50% of older normotensive people have a certain degree of RAS. RVHT is potentially curable if arterial patency is reconstituted. But hypertension and renal failure may continue or progress after treatment or after the removal of the affected kidney [(10-12)]. If revascularisation leads to amelioration of the disease, a diagnosis of RVHT can be made retrospectively [(10-12)].

Atherosclerosis is typical at the vessel origin and proximal renal artery. In 90–95% of cases and is primarily seen in patients over 55 years of age, and men more than women. Fibromuscular dysplasia (FMD) is another cause of RVHT. In distinction to atherosclerosis, this arteriopathy is more common in women and younger patients (average age, 35 years) [(11, 12)]. FMD occurs in the distal two-thirds of the artery and can be in intrarenal vessels. Multifocal stenosis is more common than unifocal RAS.

The main goal of imaging in diagnosis of RAS is to detect a potentially curable lesion in a normal-sized kidney. Doppler ultrasound is established as the initial imaging method for screening, diagnosis and follow-up after treatment of renal artery stenosis. Doppler should be used to analyse the main renal artery and intrarenal arteries. Obesity and excessive air in the bowel may hinder visualisation of the main renal artery. More than 25% of people have more than one renal artery on one or both sides [(1, 2)].

The most important duplex finding of RAS is focal elevation of PSV at the site of stenosis. The usual threshold value for diagnosis is PSV of more than 1.8–2 m/s. It is also important to evaluate the renal aortic ratio, a ratio of highest PSV at the site of stenosis divided by the PSV of the aorta at the level of the renal arteries; RAR >3.5 is considered to be diagnostic for RAS [Figure 11 and 12] [(2, 15)]. Significant stenotic lesions also produce post-stenotic turbulence.

Figure 11 Spectrum at the site of ostial, severe stenosis of the right renal artery with peak systolic velocity of 4.1 m/s, end-diastolic velocity of 1 m/s (a). High velocities in a renal artery from a lateral approach. Flow is towards the beam and no angle correction is made since its effect on measured velocity is negligible. The high

velocities and depth require high pulse repetition frequency, HPRF, scanning where there are two sample volumes (yellow arrows) displayed. Peak velocity is 3.5m/s (b).

a

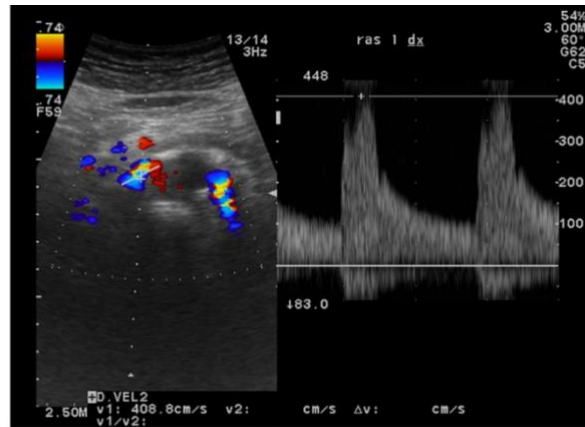


Figure 11.

b

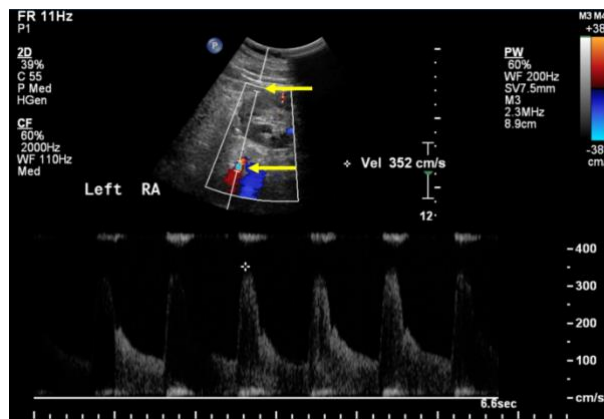
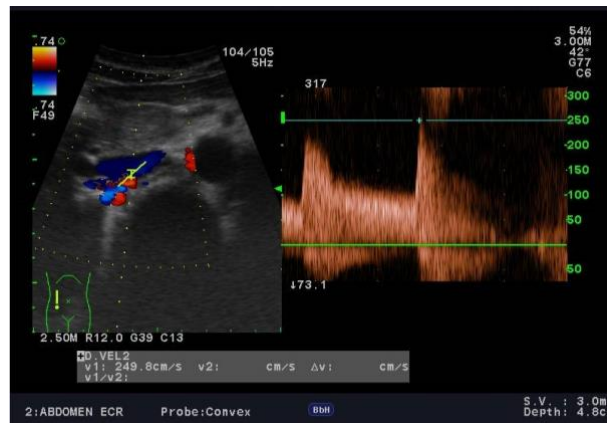


Figure 12 Doppler spectrum at the site of stenosis in the middle segment of the right renal artery in 36-year-old female with fibromuscular dysplasia of renal artery. PSV = 2.5 m/s (a). The same patient, typical finding of FMD of the right renal artery with digital subtraction angiography (b).

a



b



Demonstration of abnormal waveforms in intrarenal arteries is technically much easier compared with the main arteries, and can usually be performed even in very obese patients. Beyond significant stenoses, tardus parvus, blunted waveforms can be identified in the spectral Doppler of intrarenal arteries [(1, 2)]. These waveforms have prolonged acceleration time (greater than 0.07 s). Using higher thresholds of .09-.12 s increases specificity. Tardus parvus waveforms also increased diastolic flow [Figure 13] and prolonged AI (greater than 3 m/s/s). Comparison of Doppler and angiographic findings has demonstrated that tardus parvus spectra are seen in high-degree stenosis, above 70% or 80% [(15)]. Disappearance of *tardus parvus* spectra is observed after successful percutaneous transluminal angioplasty (PTA) or stenting of renal arteries or both [(16)]. *But tardus parvus* spectra are not always sensitive and they may not be present in cases of reduced compliance of the blood vessel, even in high-degree RAS. Decreased diastolic flow, rather than the increased flow in tardus parvus has been

proposed to predict inadequate revascularization due to irreversible changes of the kidney vasculature. If intrarenal RI is above 0.80, endovascular recanalisation may not successful [(17, 18)].

Figure 13 Post-stenotic *parvus-tardus* spectra in interlobar intrarenal artery in a case of high-degree stenosis of the main renal artery

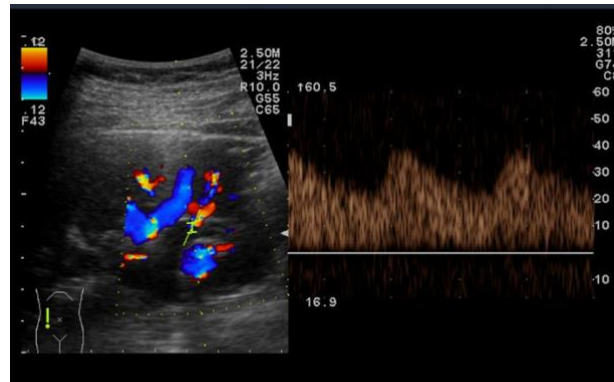


Figure 13.

Figure 14 Intrarenal interlobar post-stenotic *parvus-tardus* spectrum in 33-year-old patient with fibromuscular dysplasia and high-degree stenosis of the renal artery; prolonged acceleration time of $\Delta t=0.16$ s is seen (normal, <0.07 s) (a). Intrarenal interlobar spectrum in the same patient after the successful percutaneous transluminal angioplasty of renal artery stenosis; spectrum morphology is completely normal after the procedure (b).

a

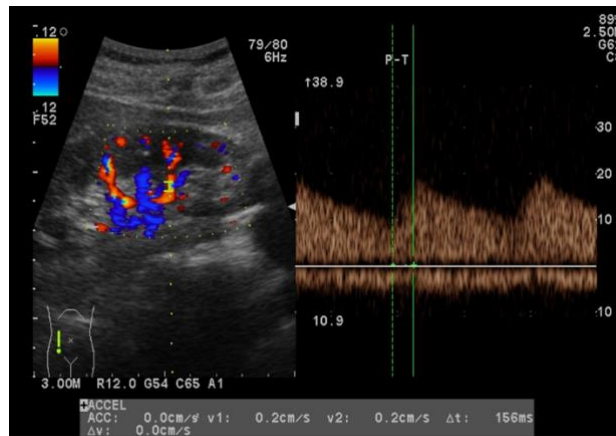


Figure 14a.

b



Figure 14b.

Accuracy of duplex Doppler ultrasound in RAS is 80–90%, which depends on the experience of the examiner and the quality of the equipment [(15)]. Although the stenosis of the accessory renal artery should be sought, it has been shown that the prevalence of isolated significant stenosis of the accessory artery is only 1.5%, absence of their detection does not decrease the usefulness of Doppler [(19)]. CT angiography has a very high negative predictive value (<95%) in diagnosis of RAS [(20)]. Contrast-enhanced MR angiography has many advantages and high diagnostic accuracy, but it has relatively low specificity and tends to overestimate moderate stenosis. There is also a risk of nephrogenic systemic fibrosis in patients with pre-existing azoemia with some, but not all, classes of gadolinium contrast media [(21, 22)]. The American College of Cardiology recommends duplex Doppler as the initial imaging method to diagnose RAS (class I, level of evidence B). CTA or MRA may be indicated after Doppler [(23)].

Doppler is important to evaluate successfulness of endovascular therapy and in follow-up to diagnose restenosis after PTA or stenting or both of the renal artery [Figure 15]. High in-stent PSV, >2 m/s indicates high-risk of impaired stent patency and loss of renal function [(24)].

Figure 15 Flow through the stent in the left renal artery with colour Doppler and spectrum that demonstrates normal velocity (PSV = 71 cm/s).

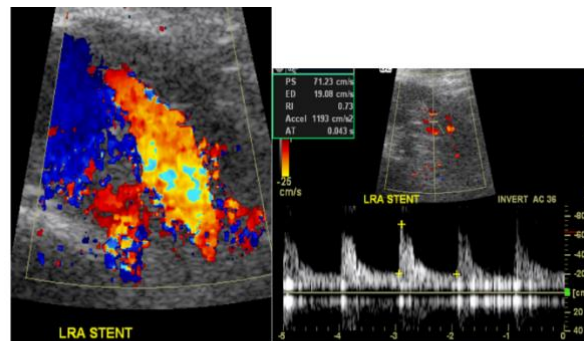


Figure 15.

Clinical scenario

The analysis of the natural history of untreated atherosclerotic RAS has established that 42–49% of stenotic renal artery progress during 6–24 months, and angiographic or ultrasound follow-up has shown that 11–14% of RAS progress to occlusion [(25, 26)]. Patients surviving 15 years with end-stage renal disease because of RAS is 0%, but 32% in patients with end-stage renal disease for other reasons (*e.g.* autosomal dominant polycystic kidney disease) [(27)]. More than 80% of patients have good blood pressure control with medical therapy. Surgical revascularisation has relatively high mortality and post-operative complication rate [(28)]. Regarding endovascular revascularisation, percutaneous transluminal angioplasty is an excellent method for the treatment of fibromuscular dysplasia, where results are much better than in atherosclerotic disease. The best treatment for atherosclerotic RAS is controversial, and conflicting data have been published regarding indications, benefits, complications and advantages of endovascular over medical therapy [(28-32)]. Although 25–30% of patients with

impaired renal function can recover glomerular filtration after endovascular revascularisation, many have no apparent change in renal function, and 19–25% experience a significant loss of kidney function, some as a result of atheroemboli [(31)]. A review of RAS treatment in 2006 for the Agency for Healthcare Research and Quality concluded that there is insufficient evidence to suggest a clear advantage of renal revascularisation over maximal medical therapy [(27)].

A study comparing percutaneous revascularisation vs. medical therapy for renal-artery stenosis is the ASTRAL study [(33)]. 806 patients with atherosclerotic high-degree RAS were randomised into groups that underwent revascularisation in addition to receiving medical therapy, and into a group receiving medical therapy alone. The primary outcome was renal function and the secondary outcomes were blood pressure, time to renal and major cardiovascular events, and mortality. During a mean follow-up of 34 months there was no evidence of a worthwhile clinical benefit from revascularisation in patients with atherosclerotic renovascular disease, while serious complications associated with revascularisation occurred in 23 of the 403 treated patients.

In conclusion, the decision to revascularize is a difficult one. There is ongoing research to identify subgroups of patients with RAS who may benefit from endovascular/surgical intervention [(34)]. Evaluating renal size and parenchymal disease should be evaluated and followed by ultrasound. Doppler ultrasound should be the first imaging modality to diagnose RAS. Main renal and intrarenal evaluation both have advantages (accuracy for main evaluation and ease for intrarenal evaluation). Meticulous evaluation of intrarenal spectra should be performed to identify those patients that may not benefit from revascularisation. If ultrasound findings are equivocal, CT angiography can be performed; and it has very high negative predictive value. Contrast-enhanced MR angiography has a high diagnostic accuracy, but it has relatively low specificity and tends to overestimate moderate stenosis.

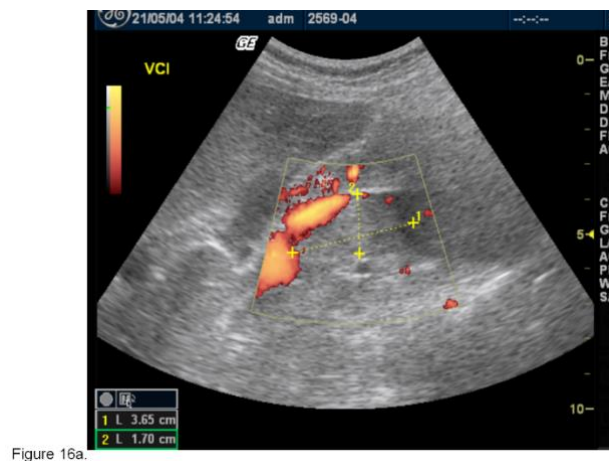
Renal vein thrombosis

Doppler is very accurate in the diagnosis of renal vein thrombosis. Colour Doppler can directly visualise a distended vein, filled with the thrombus, without flow. In adults, renal vein thrombosis is most commonly seen in patients with kidney cancer that commonly infiltrates the renal vein and inferior vena cava. In these patients, malignant venous thrombus may

demonstrate vascularisation on colour Doppler. Indirect signs of RVT may be an alteration of intrarenal arterial spectra, with extreme elevation of RI due to intrarenal oedema caused by impaired venous drainage [(35)]. RVT that is not caused by a malignant tumour is more common on the left side, presumably since the left renal vein is longer than the right one and narrowed by the SMA. In adults RVT may be caused by nephrotic syndrome, hypercoagulable conditions, oral contraceptive intake (Figure 16a-c), trauma, retroperitoneal fibrosis and thrombophlebitis migrans. In children more common causes are dehydration and trauma. Early diagnosis is important because to ensure adequate therapy. Venous recanalisation after successful treatment may be evaluated by colour duplex Doppler.

Figure 16 Echogenic thrombus that protrudes from the right renal artery into the inferior vena cava (a). Intrarenal arterial spectrum from the right kidney demonstrates very high resistance due to the right renal vein thrombosis; intrarenal arterial resistance is elevated due to oedema caused by the impaired venous drainage (b). (c). After the successful recanalisation of right renal vein thrombosis normal spectra are visible in intrarenal arteries, with normal resistance and RI =0.61.

a



b

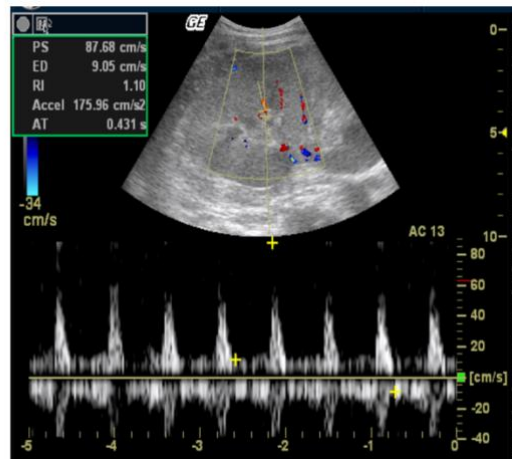


Figure 16b.

C

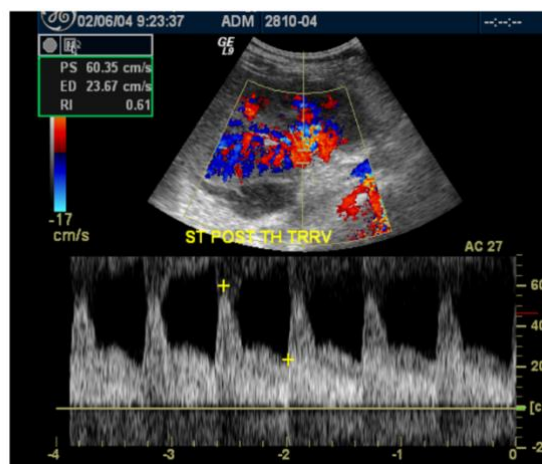
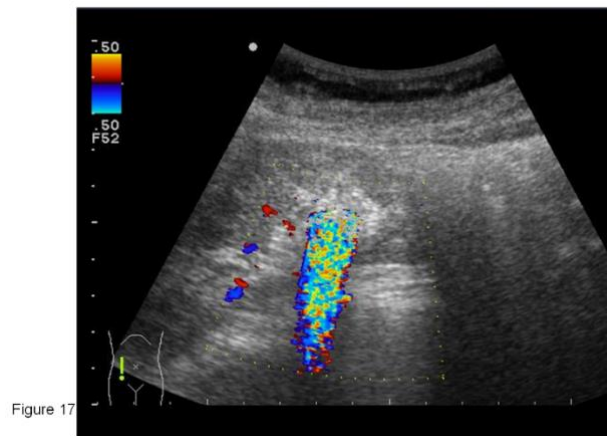


Figure 16c.

Doppler in diagnosis of other renal diseases

Colour Doppler is useful to diagnose small renal stones due to “twinkling” artefacts unrelated to blood flow; mosaic color appears in the stone shadow from irregularities of the stone surface [Figure 17]. This artefact is usually not seen in stones composed of calcium-oxalate [(36)].

Figure 17 Twinkling artefact behind a renal stone that does not cause collecting system dilatation.



Conventional ultrasound cannot differentiate obstructive and non-obstructive renal collecting system dilatation. Doppler can demonstrate elevated renal vascular resistance in significant obstruction of the collecting system. RVR is increased due to several vasoconstrictor substances, principally thromboxane A-2. It is important to measure RI in intrarenal arteries of both kidneys and a difference in RI of 0.08 or more is indicative of significant unilateral obstruction [Figure 18a,b] [(7, 37)]. RI is usually elevated within 6–48 h after the onset of obstruction.

Figure 18 Elevated renal vascular resistance in the obstructed right kidney due to the ureteric stone. RI=0.74. Normal RI in a non-obstructed left kidney of the same patient. RI=0.60, dRI= 0.14 (b).

a

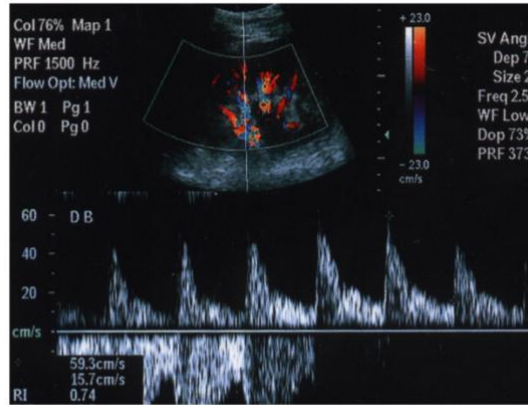


Figure 18a.

b

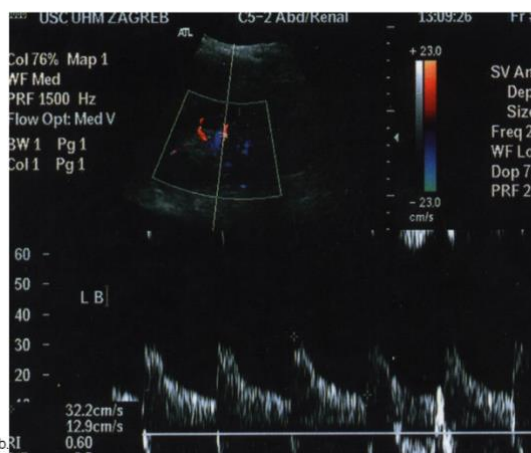


Figure 18b.

One might also analyse ureteric jets with colour Doppler [Figure 19]; these are short-lasting jets of urine entering the bladder from the ureters that indicates patent ureter [(38)].

Figure 19 Ureteral jets visible from both vesicoureteric orifices. They are helpful to locate orifices and measure their distance to the midline of the bladder.

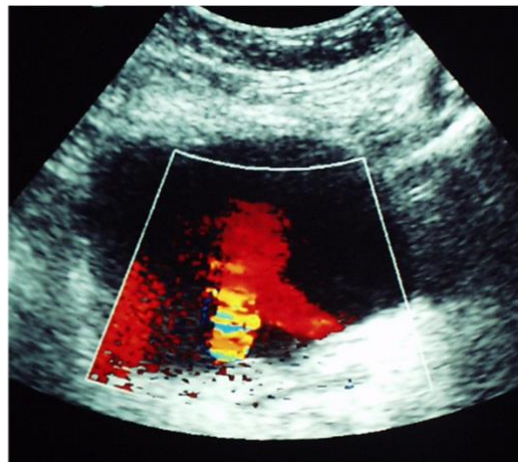


Figure 19.

Renal vascular resistance and intrarenal RIs are elevated in acute kidney injury (AKI) and in several renal parenchymal diseases, particularly those with pathological changes in tubules, renal interstitium and blood vessels. Patients with isolated glomerular lesions usually have normal RIs [(1, 39)]. Using renal resistance as a marker for AKI and/or progression of disease is an active area of investigation [(40)].

Haemolytic-uraemic syndrome causes acute renal failure in children. Its main feature is thrombotic microangiopathy and pronounced intrarenal vasoconstriction, with subsequent elevation of RVR. Children with HUS have elevated renal RIs. Restitution of renal function may be expected if RI values normalise in the diuretic phase of the disease, and changes in RI occur before changes in laboratory or radionuclide findings and clinical signs of improvement. Doppler can therefore be used to stop haemodialysis treatment [(41)].

Acute renal failure (ARF) is caused by many diseases that need to be differentiated to ensure adequate treatment. Doppler may be useful to differentiate two of the most common causes of ARF: acute pre-renal failure and acute tubular necrosis (ATN). In ATN, RI above 0.75 is observed in more than 90% of patients, while in the acute pre-renal failure RI values are usually normal [(41, 42)]. An example of very elevated resistance in patients with ARF caused by ATN is demonstrated in [Figure 20].

Figure 20 High intrarenal arterial resistance (RI=0.81) in patients with the acute renal failure due to the acute tubular necrosis.

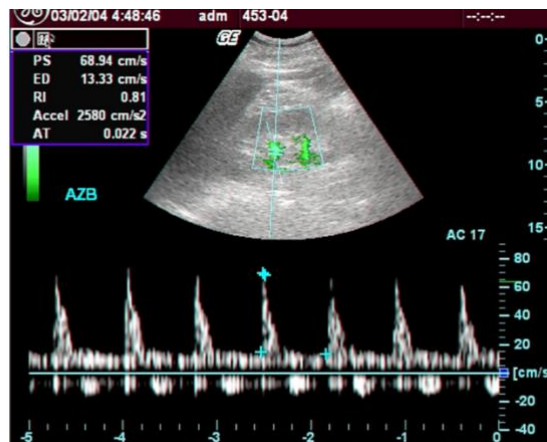


Figure 20.

Diabetic nephropathy is very common and the leading cause of chronic renal failure. Histopathological changes in the diabetic kidney affect mostly blood vessels, and can be manifested as increased RVR and increased RI [Figure 21]. An increase in RI is proportional to the progression of diabetic nephropathy, but RI values over 0.70 are seen only in stages of azothaemia and clinically manifested disease; while in early stages, especially in the stage of microalbuminuria RIs are not increased [(9)]. Doppler changes are seen before conventional ultrasound changes in diabetic nephropathy [(43, 44)].

Figure 21 Elevated intrarenal arterial resistance (RI=0.73) in patients with diabetic nephropathy and non-insulin dependant diabetes mellitus.

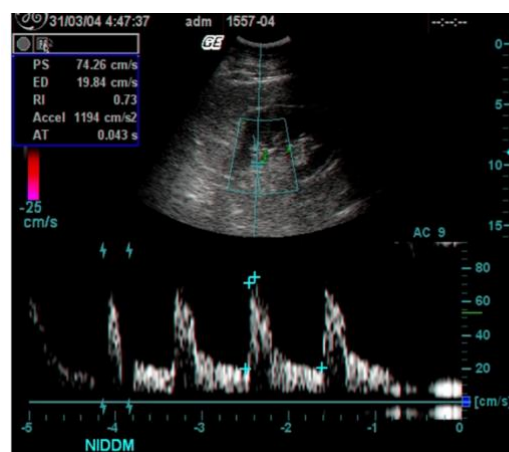


Figure 21.

Hepatorenal syndrome marks impairment of renal function in patients with chronic liver disease. These patients have intense intrarenal vasoconstriction and increased renal RI values. Elevation of RI may be observed before elevation of serum creatinine, *e.g.* before clinically proven HRS [(45)]. In patients with autosomal dominant polycystic kidney disease renal RI elevation correlates well with renal functional impairment and the degree of morphological kidney changes on conventional ultrasound [(46)]. Colour duplex Doppler is useful to evaluate vascularisation of solid renal tumours, although it does not have an important role in differentiation of various tumour types. Colour duplex Doppler is useful to guide the needle path during kidney biopsy and to detect complications of biopsy such as pseudoaneurysms [Figure 22a,b] and AV fistulas [Figure 23]. Post-biopsy AVF is usually much smaller than congenital AV malformation in the kidney [(1)].

Figure 22 Colour Doppler of the part of the kidney after biopsy. Iatrogenic pseudoaneurysm with colour-coded flow in both directions (a). Spectral display of the same pseudoaneurysm with the flow above and below the baseline (b).

a



b

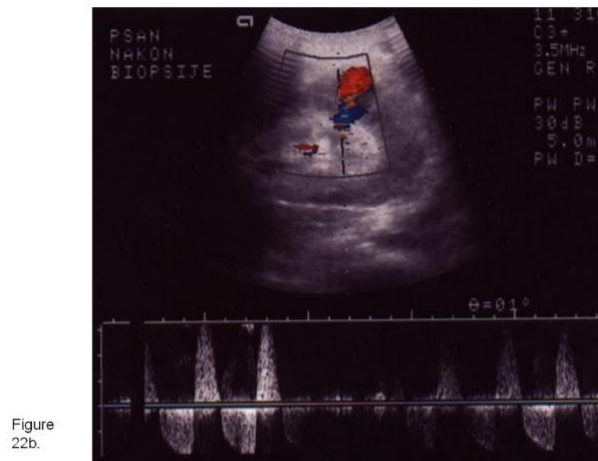


Figure 22b.

Figure 23 High systolic and high diastolic flow Doppler spectrum from iatrogenic arteriovenous fistula in the kidney, which is a complication of kidney biopsy.

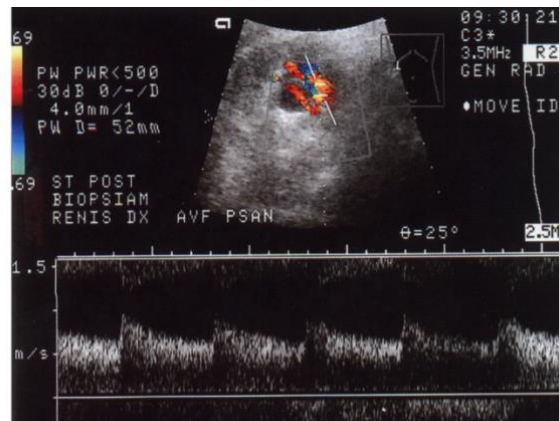


Figure 23.

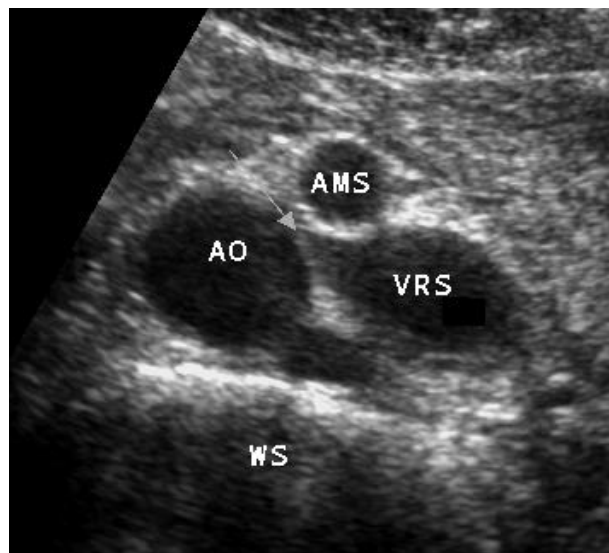
Colour and power Doppler are useful in acute pyelonephritis, especially in children, in which focal area of hypovascularisation can be demonstrated with high accuracy of 80–90%, and avoids methods that expose children to ionizing radiation, such as dynamic scintigraphy and CT [(47)].

Figure 24 Colour duplex Doppler of elevated renal vascular resistance in a 60-year-old female patient with autosomal dominant polycystic kidney disease; RI is 0.76.

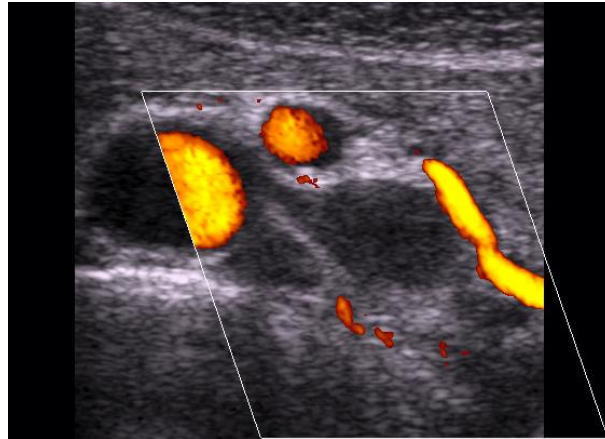


Figure 25 Nutcracker syndrome. B-mode (a) and Power Doppler (b). The left renal vein (VRS) is between the aorta (19) and superior mesenteric artery (AMS). The vertebral spine is also indicated (WS). VCI: inferior vena cava. Niere: kidney.

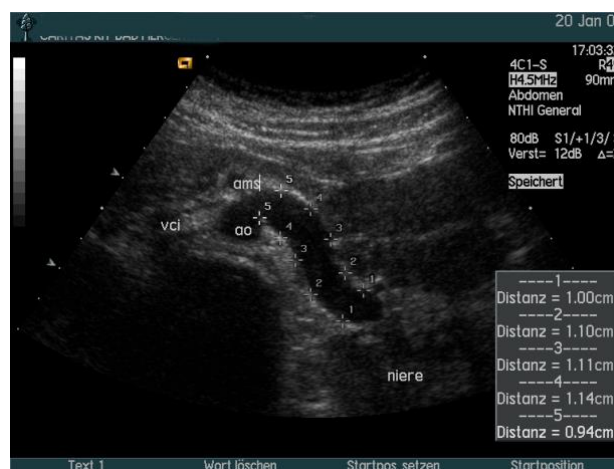
a



b



C



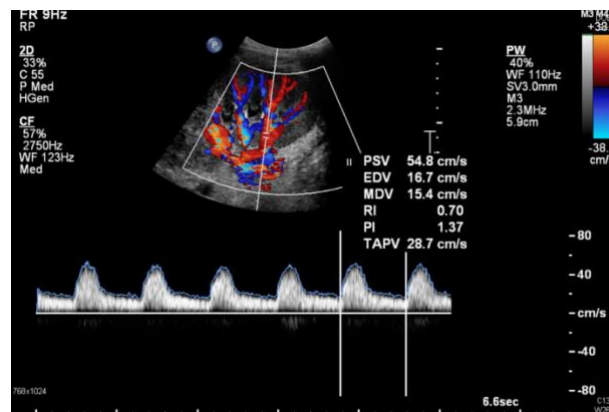
Renal Transplants

Colour Doppler imaging of renal transplants is, in comparison with native kidneys, relatively straightforward. The kidney lies in the iliac fossa and is usually superficial. The vascular anatomy including the presence of multiple arteries can be obtained from the operative note. Doppler ultrasound complements B-mode ultrasound in the investigation of poor function or changes in graft function. It is most useful when investigating vascular causes of poor function, graft artery stenosis, renal vein thrombosis or arteriovenous fistula. It is not specific when examining flow changes as a result of rejection, drug toxicity and acute tubular necrosis.

Scanning kidney transplants

Higher frequency curvilinear arrays (2-9 MHz) are suitable to image the renal transplant and the main arteries and veins. In slim patients, low frequency linear arrays (4-9 MHz) may be helpful to if the iliac arteries are superficial. The intrarenal flow arterial waveforms are measured in the upper pole, mid graft and lower pole. In the early post-transplant period, rapid changes in the vascular resistance can occur. It may be advantageous to use the pulsatility index (PI) as a measure of resistance. If there is zero flow at any point in the cardiac cycle $RI = 1$ but PI discriminates between a waveform with no diastolic flow and one where diastolic flow falls below zero. The range for normal flow waveforms is wider than for a native kidney. While a normal flow waveform usually has PIs in the range 0.8 -1.5, ($RI = 0.6 - 0.75$) there are transplants with good long-term function with higher PIs. A change in flow waveform shape is a more important indication of changing RVR [Figure 26].

Figure 26 The colour image shows several segmental and interlobar arteries and veins. Flow indices are in the normal range of RI and PI.

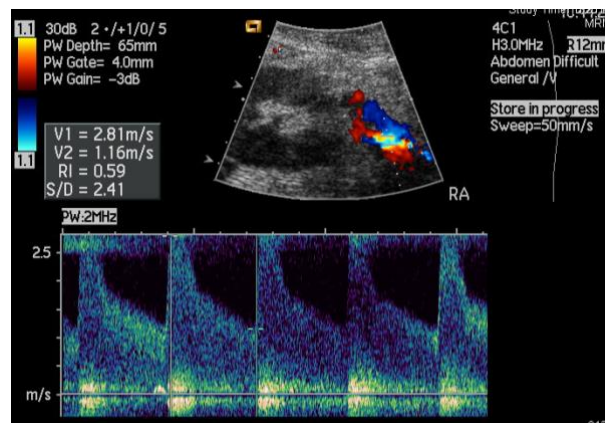


Arterial stenosis

The iliac artery should be investigated to ensure no proximal stenosis. The normal external iliac artery waveform has high acceleration and a multiphasic pattern. Damped flow in the

external of iliac artery is indicative of proximal disease which can be confirmed by direct imaging of the upstream stenosis. The renal artery is imaged from anastomosis to hilar level. The range of flow velocities is higher than in native kidneys and local changes at points of tight curvature can be confusing. PSV ratios of ≥ 2.5 or over are indicative of stenosis as are PSVs of ≥ 2.5 m/s [(48)] [Figure 27]. Intrarenal flow waveforms are less helpful than for native kidneys because of the various factors that affect intrarenal flow waveforms. However, severely damped flow waveforms are indicative of upstream stenosis.

Figure 26 Aliasing in a renal artery indicates raised velocities. Uncorrected peak velocity is 2.8 m/s, correcting the beam/flow angle will increase this measurement.

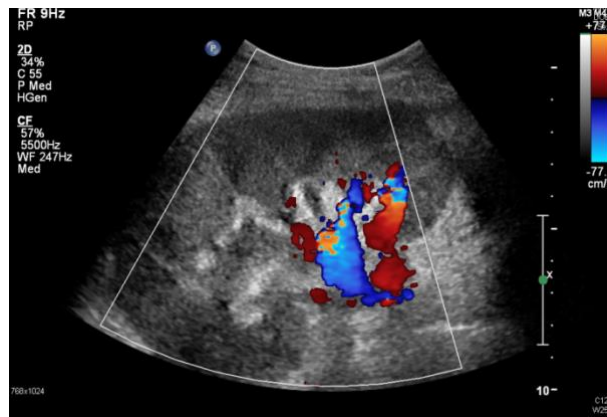


Arteriovenous fistula

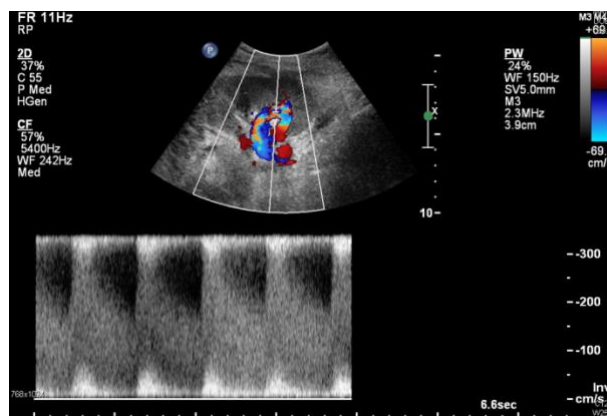
A-V fistulas may be found post-biopsy. The appearance is of high velocity disturbed flow at the site of the fistula [Figure 28] with high velocity low resistance flow in the artery supplying the fistula and arterial pulsations during systole in the vein draining it. Fistulas present a risk if further biopsy is undertaken at the same site. Fistulas are occasionally associated with pseudoaneurysm and may produce or worsen hypertension.

Figure 27 Colour image (a) and spectral Doppler (b) of flow through an AV fistula. The high colour scale shows the arterial supply and venous drainage. The Doppler waveform shows high velocity disturbed flow.

a



b



Venous thrombosis

Renal vein thrombosis most frequently occurs in the early post-operative period. Doppler flows no venous signals. Arterial waveforms show sharp systolic peaks and reversed flow in diastole ("to and fro" sign).

Flow changes in rejection

An increase in intrarenal flow waveform resistance between visits as measured by PI or RI is a cause for concern as it is an early sign of rejection. Absolute values vary considerably in the immediate post-transplantation period, high resistance flow waveforms are also seen in cases of acute tubular necrosis, especially if there has been a comparatively long ischemic period before transplantation. The complex post-transplantation course may also include drug nephrotoxicity which has also been associated with an increase in PI/RI. Changes in flow waveforms have been shown to lack sensitivity or specificity for rejection but are still useful as an indication of changes in renovascular resistance which merits further investigation. Early acute tubular necrosis is often associated with increases in edema. Changes in arterial flow waveform shape are sometimes accompanied by high intrarenal venous velocities caused by extrinsic compression on the low pressure veins. Chronic rejection is manifest by a steady reduction in arterial velocities throughout the kidney which may be accompanied by a slight rise in PI. These changes are irreversible and are presaged by changes in renal function.

References

1. Pellerito JS, Zwiebel WJ: Ultrasound assessment of native renal vessels and renal allografts. In: Zwiebel WJ, Pellerito JS, eds. *Introduction to Vascular Ultrasonography*. Philadelphia: Elsevier, 2005; 612-636.
2. Platt JF. Doppler ultrasound of the kidney. *Semin Ultrasound CT MR* 1997;18:22-32.
3. Fernbach SK, Feinstein KA: Normal renal anatomy, variants and congenital anomalies. In: Slovis TL, ed. *Caffey's Pediatric Diagnostic Imaging, 11th ED*. Philadelphia: Elsevier, 2007; 2234-2235.
4. Meissner MH, Khilnani NM, Labropoulos N, Gasparis AP, Gibson K, Greiner M, Learman LA, et al. The Symptoms-Varices-Pathophysiology classification of pelvic venous disorders: A report of the American Vein & Lymphatic Society International Working Group on Pelvic Venous Disorders. *J Vasc Surg Venous Lymphat Disord* 2021;9:568-584.
5. Brkljacic B, Drinkovic I. Age-related changes of renal vascular resistance in normal native kidneys: color duplex Doppler US assessment. *Radiol Oncol* 1995;29:102-106.
6. Knapp R, Plotzeneder A, Frauscher F, Helweg G, Judmaier W, zur Nedden D, Recheis W, et al. Variability of Doppler parameters in the healthy kidney: an anatomic-physiologic correlation. *J Ultrasound Med* 1995;14:427-429.
7. Brkljacic B, Kuzmic AC, Dmitrovic R, Rados M, Vidjak V. Doppler sonographic renal resistance index and resistance index ratio in children and adolescents with unilateral hydronephrosis. *Eur Radiol* 2002;12:2747-2751.
8. Sigirci A, Hallac T, Akyncy A, Temel I, Gulcan H, Aslan M, Kocer M, et al. Renal interlobar artery parameters with duplex Doppler sonography and correlations with age,

plasma renin, and aldosterone levels in healthy children. *AJR Am J Roentgenol* 2006;186:828-832.

9. Brkljacic B, Mrzljak V, Drinkovic I, Soldo D, Sabljari-Matovinovic M, Hebrang A. Renal vascular resistance in diabetic nephropathy: duplex Doppler US evaluation. *Radiology* 1994;192:549-554.
10. Brkljacic B. Renovascular disease. *Eur Radiol* 2009;19 (Suppl 1):S18.
11. Spargo BH, Baas M: The kidney - vascular diseases. In: Rubin E, Farber JL, eds. *Pathology*. Philadelphia: JB Lippincott Company, 1994; 851-858.
12. Rosenfield K, Jaff MR. An 82-year-old woman with worsening hypertension: review of renal artery stenosis. *JAMA* 2008;300:2036-2044.
13. Edwards MS, Craven TE, Burke GL, Dean RH, Hansen KJ. Renovascular disease and the risk of adverse coronary events in the elderly: a prospective, population-based study. *Arch Intern Med* 2005;165:207-213.
14. White CJ, Jaff MR, Haskal ZJ, Jones DJ, Olin JW, Rocha-Singh KJ, Rosenfield KA, et al. Indications for renal arteriography at the time of coronary arteriography: a science advisory from the American Heart Association Committee on Diagnostic and Interventional Cardiac Catheterization, Council on Clinical Cardiology, and the Councils on Cardiovascular Radiology and Intervention and on Kidney in Cardiovascular Disease. *Circulation* 2006;114:1892-1895.
15. Brkljacic B: Renal Artery Stenosis and Renovascular Hypertension. In: Brkljacic B, ed. *Vascular Ultrasound*. Zagreb: Medicinska naklada, 2010; 268-274.
16. Brkljacic B, Hebrang A, Drinkovic I. Duplex Doppler ultrasound of intrarenal arteries in the assessment of the percutaneous transluminal angioplasty of renal artery stenosis – a case report. *Radiol Oncol* 1996;30:9-13.
17. Radermacher J, Chavan A, Bleck J, Vitzthum A, Stoess B, Gebel MJ, Galanski M, et al. Use of Doppler ultrasonography to predict the outcome of therapy for renal-artery stenosis. *N Engl J Med* 2001;344:410-417.
18. Crutchley TA, Pearce JD, Craven TE, Stafford JM, Edwards MS, Hansen KJ. Clinical utility of the resistive index in atherosclerotic renovascular disease. *J Vasc Surg* 2009;49:148-155, 155 e141-143; discussion 155.
19. Bude RO, Forauer AR, Caoili EM, Nghiem HV. Is it necessary to study accessory arteries when screening the renal arteries for renovascular hypertension? *Radiology* 2003;226:411-416.
20. Saba L, Sanfilippo R, Montisci R, Conti M, Mallarini G. Accessory renal artery stenosis and hypertension: are these correlated? Evaluation using multidetector-row computed tomographic angiography. *Acta Radiol* 2008;49:278-284.
21. Tan KT, van Beek EJ, Brown PW, van Delden OM, Tijssen J, Ramsay LE. Magnetic resonance angiography for the diagnosis of renal artery stenosis: a meta-analysis. *Clin Radiol* 2002;57:617-624.
22. Broome DR, Girguis MS, Baron PW, Cottrell AC, Kjellin I, Kirk GA. Gadodiamide-associated nephrogenic systemic fibrosis: why radiologists should be concerned. *AJR Am J Roentgenol* 2007;188:586-592.
23. Hirsch AT, Haskal ZJ, Hertzner NR, Bakal CW, Creager MA, Halperin JL, Hiratzka LF, et al. ACC/AHA Guidelines for the Management of Patients with Peripheral Arterial Disease (lower extremity, renal, mesenteric, and abdominal aortic): a collaborative report from the American Associations for Vascular Surgery/Society for Vascular Surgery, Society for Cardiovascular Angiography and Interventions, Society for Vascular Medicine and Biology, Society of Interventional Radiology, and the ACC/AHA Task Force on Practice Guidelines

(writing committee to develop guidelines for the management of patients with peripheral arterial disease)--summary of recommendations. *J Vasc Interv Radiol* 2006;17:1383-1397; quiz 1398.

24. Girndt M, Kaul H, Maute C, Kramann B, Kohler H, Uder M. Enhanced flow velocity after stenting of renal arteries is associated with decreased renal function. *Nephron Clin Pract* 2007;105:c84-89.
25. Greco BA, Breyer JA. The natural history of renal artery stenosis: who should be evaluated for suspected ischemic nephropathy? *Semin Nephrol* 1996;16:2-11.
26. Zierler RE, Bergelin RO, Isaacson JA, Strandness DE, Jr. Natural history of atherosclerotic renal artery stenosis: a prospective study with duplex ultrasonography. *J Vasc Surg* 1994;19:250-257; discussion 257-258.
27. Balk E, Raman G, Chung M, Ip S, Tatsioni A, Alonso A, Chew P, et al. Effectiveness of management strategies for renal artery stenosis: a systematic review. *Ann Intern Med* 2006;145:901-912.
28. Zeller T. Percutaneous endovascular therapy of renal artery stenosis: technical and clinical developments in the past decade. *J Endovasc Ther* 2004;11 Suppl 2:II96-106.
29. van Jaarsveld BC, Krijnen P, Pieterman H, Derkx FH, Deinum J, Postma CT, Dees A, et al. The effect of balloon angioplasty on hypertension in atherosclerotic renal-artery stenosis. Dutch Renal Artery Stenosis Intervention Cooperative Study Group. *N Engl J Med* 2000;342:1007-1014.
30. Ives NJ, Wheatley K, Stowe RL, Krijnen P, Plouin PF, van Jaarsveld BC, Gray R. Continuing uncertainty about the value of percutaneous revascularization in atherosclerotic renovascular disease: a meta-analysis of randomized trials. *Nephrol Dial Transplant* 2003;18:298-304.
31. Textor SC. Ischemic nephropathy: where are we now? *J Am Soc Nephrol* 2004;15:1974-1982.
32. Salifu MO, Haria DM, Badero O, Aytug S, McFarlane SI. Challenges in the diagnosis and management of renal artery stenosis. *Curr Hypertens Rep* 2005;7:219-227.
33. Wheatley K, Ives N, Gray R. ASTRAL Investigators. Revascularization versus medical therapy for renal artery stenosis. *N Engl J Med* 2009;361:1953-1962.
34. Textor SC, Taler SJ. Rediscovering Renovascular Hypertension. *Hypertension* 2019;74:1297-1299.
35. Platt JF, Ellis JH, Rubin JM. Intrarenal arterial Doppler sonography in the detection of renal vein thrombosis of the native kidney. *AJR Am J Roentgenol* 1994;162:1367-1370.
36. Lee JY, Kim SH, Cho JY, Han D. Color and power Doppler twinkling artifacts from urinary stones: clinical observations and phantom studies. *AJR Am J Roentgenol* 2001;176:1441-1445.
37. Brkljacic B, Drinkovic I, Sabljari-Matovinovic M, Soldo D, Morovic-Vergles J, Vidjak V, Hebrang A. Intrarenal duplex Doppler sonographic evaluation of unilateral native kidney obstruction. *J Ultrasound Med* 1994;13:197-204.
38. de Bessa J, Jr., Denes FT, Chammas MC, Cerri L, Monteiro ED, Buchpiguel CA, Cerri GG, et al. Diagnostic accuracy of color Doppler sonographic study of the ureteric jets in evaluation of hydronephrosis. *J Pediatr Urol* 2008;4:113-117.
39. Coley BD, Brkljacic B. Renal Failure and Transplantation. In: Slovic T, editor. *Caffey's Pediatric Diagnostic Imaging*, 11th Ed. Philadelphia: Elsevier; 2007. p. 2311-2324.
40. Kelahan LC, Desser TS, Troxell ML, Kamaya A. Ultrasound Assessment of Acute Kidney Injury. *Ultrasound Q* 2019;35:173-180.

41. Patriquin HB, O'Regan S, Robitaille P, Paltiel H. Hemolytic-uremic syndrome: intrarenal arterial Doppler patterns as a useful guide to therapy. *Radiology* 1989;172:625-628.
42. Mucelli RP, Bertolotto M. Imaging techniques in acute renal failure. *Kidney Int Suppl* 1998;66:S102-105.
43. Soldo D, Brkljacic B, Bozikov V, Drinkovic I, Hauser M. Diabetic nephropathy. Comparison of conventional and duplex Doppler ultrasonographic findings. *Acta Radiol* 1997;38:296-302.
44. Quaia E, Correas JM, Mehta M, Murchison JT, Gennari AG, van Beek EJR. Gray Scale Ultrasound, Color Doppler Ultrasound, and Contrast-Enhanced Ultrasound in Renal Parenchymal Diseases. *Ultrasound Q* 2018;34:250-267.
45. Platt JF, Ellis JH, Rubin JM, Merion RM, Lucey MR. Renal duplex Doppler ultrasonography: a noninvasive predictor of kidney dysfunction and hepatorenal failure in liver disease. *Hepatology* 1994;20:362-369.
46. Brkljacic B, Sabljari-Matovinovic M, Putarek K, Soldo D, Morovic-Vergles J, Hauser M. Renal vascular resistance in autosomal dominant polycystic kidney disease. Evaluation with color Doppler ultrasound. *Acta Radiol* 1997;38:840-846.
47. Riccabona M, Ring E, Schwinger W, Aigner R. Amplitude coded-colour Doppler sonography in paediatric renal disease. *Eur Radiol* 2001;11:861-866.
48. Baxter GM, Ireland H, Moss JG, Harden PN, Junor BJ, Rodger RS, Briggs JD. Colour Doppler ultrasound in renal transplant artery stenosis: which Doppler index? *Clin Radiol* 1995;50:618-622.